

# 1 Effect of Sec61 interaction with Mpd1 2 on Endoplasmic Reticulum- 3 Associated Degradation

4 **Fábio Pereira<sup>1</sup>, Mandy Rettel<sup>2</sup>, Frank Stein<sup>2</sup>, Mikhail M. Savitski<sup>2</sup>, Ian Collinson<sup>3</sup>,**  
5 **Karin Römisch<sup>1\*</sup>**

\*For correspondence:  
[k.roemisch@mx.uni-saarland.de](mailto:k.roemisch@mx.uni-saarland.de)  
(+49 681 3022704)

6 <sup>1</sup>Faculty of Natural Sciences and Technology, Saarland University, Saarbrücken;  
7 <sup>2</sup>Proteomics Core Facility, EMBL, Heidelberg; <sup>3</sup>School of Biochemistry, University of  
8 Bristol, Bristol

---

## 10 Abstract

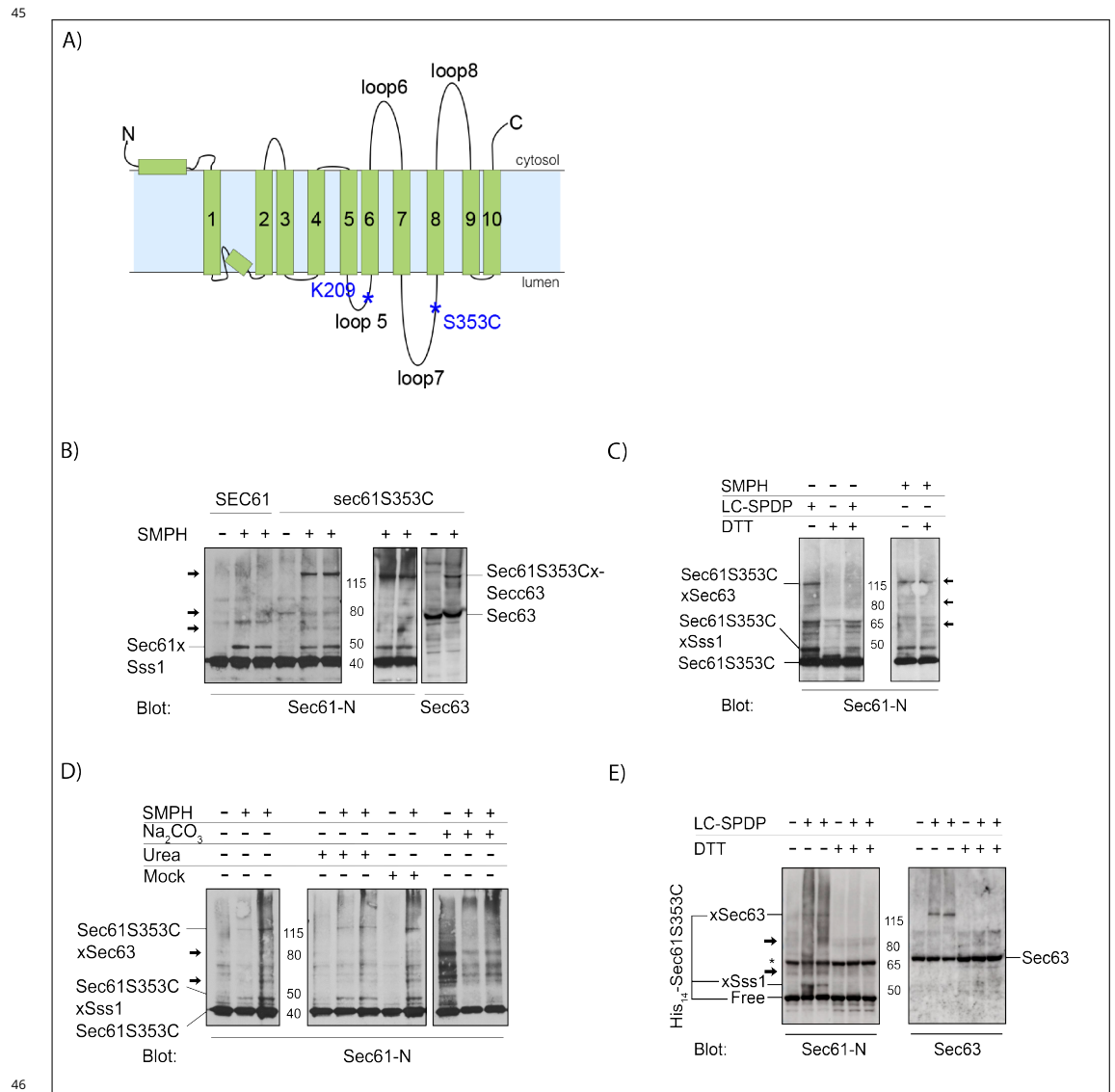
11 Proteins that misfold in the endoplasmic reticulum (ER) are transported back to the cytosol for  
12 ER-associated degradation (ERAD). The Sec61 channel is one of the candidates for the retrograde  
13 transport conduit. Channel opening from the ER lumen must be triggered by ERAD factors and  
14 substrates. Here we identified new luminal interaction partners of Sec61 by chemical crosslinking  
15 and mass spectrometry. In addition to known Sec61 interactors we detected ERAD factors including  
16 Cue1, Ubc6, Ubc7, Asi3, and Mpd1. We show that the CPY\* ERAD factor Mpd1 binds to the luminal  
17 Sec61 hinge region. Deletion of the Mpd1 binding site reduced the interaction between both  
18 proteins and caused an ERAD defect specific for CPY\* without affecting protein import into the ER  
19 or ERAD of other substrates. Our data suggest that Mpd1 binding to Sec61 is a prerequisite for  
20 CPY\* ERAD and confirm a role of Sec61 in ERAD of misfolded secretory proteins.

---

## 22 Introduction

23 In eukaryotes about 30% of all proteins constitute secretory pathway cargo (*Ghaemmaghami et al.,*  
24 *2003*). These proteins are transported into the ER by the conserved heterotrimeric Sec61 channel  
25 formed by Sec61, Sbh1, and Sss1 in yeast (Sec61 $\alpha$ , Sec61 $\beta$ , Sec61 $\gamma$  in mammals) (*Johnson and van*  
26 *Waes, 1999*). During targeting and translocation the Sec61 channel interacts with multiple other  
27 protein complexes on its cytosolic face and in the ER membrane such as the ribosome, the SRP  
28 receptor, the Sec63 complex, oligosaccharyl transferase, and signal peptidase (*Kalies et al., 1994;*  
29 *Brodsky et al., 1995; Jadhav et al., 2015; Scheper et al., 2003; Kalies et al., 1998*). If proteins fail to  
30 fold in the ER, they trigger the Unfolded Protein Response (UPR), unless they are transported back  
31 to the cytosol for ERAD (*Pilla et al., 2017; Römisch, 2017*). Although this process has been intensely  
32 studied for over 20 years, the identity of the retrograde transport channel is still controversial. The  
33 first and most investigated candidate is the Sec61 channel (*Römisch, 2017*). The E3 ubiquitin ligase  
34 Hrd1 and the pseudorhomboid proteases Der1 and Dfm1 have been proposed more recently as  
35 ERAD channels (*Mehnert et al., 2014; Neal et al., 2018*). The Sec61 channel has been shown to  
36 interact with Hrd1, and Hrd1 with Der1, so these proteins may also operate together in transporting  
37 ERAD substrates to the cytosol (*Ng et al., 2007; Carvalho et al., 2006; Römisch, 2017*). If the Sec61  
38 channel were involved in retrograde transport of ERAD substrates, it would have to interact with  
39 ERAD factors targeting ERAD substrates to its luminal end. While Sec61 interaction with ERAD  
40 substrates has been shown (*Pilon et al., 1997; Schäfer and Wolf, 2009*), the only known ER luminal

41 ERAD factor that is known to interact with Sec61 is the Hsp70 BiP (*Schäuble et al., 2012*). Here we  
 42 have used chemical crosslinking and mass spectrometry to identify new interactors of Sec61 with  
 43 specific focus on ERAD-relevant and luminal interactors in order to better understand the role of  
 44 the Sec61 channel in this process.



47

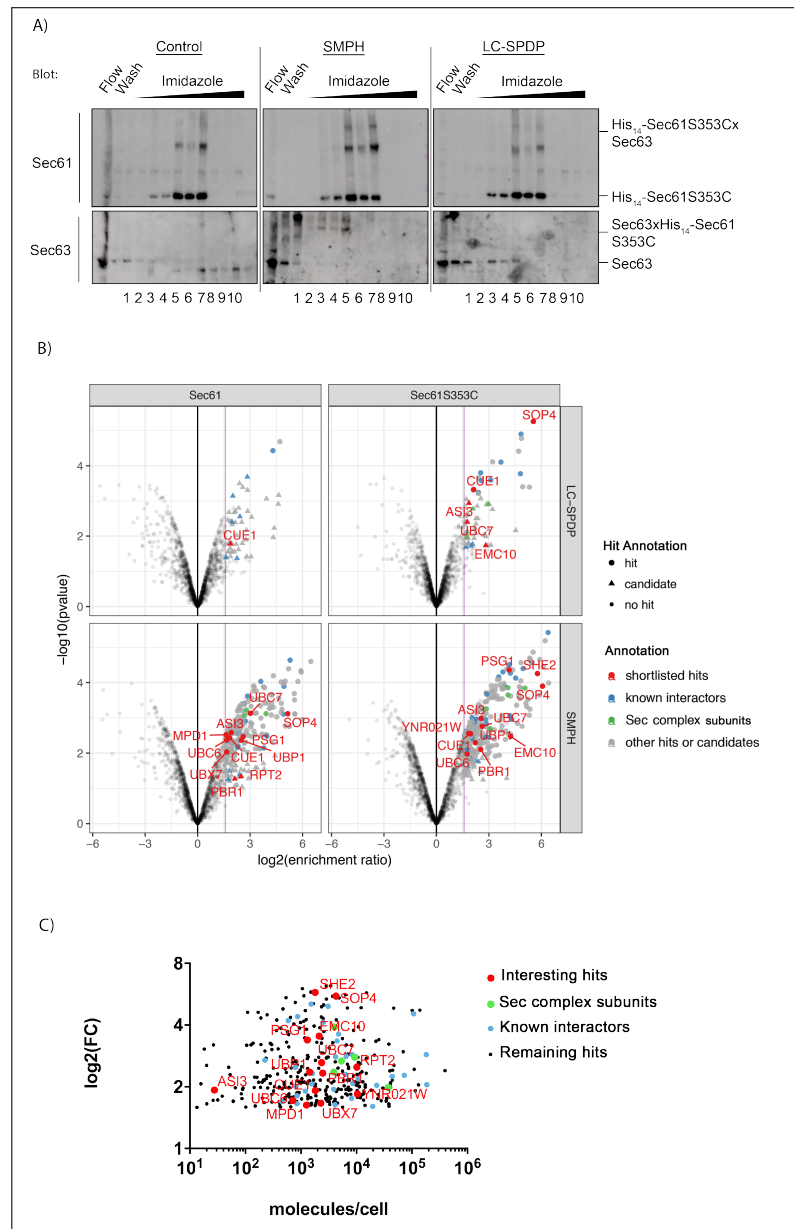
**Figure 1. Optimization of crosslinking to Sec61S353C.** **A)** Topological model of Sec61. **B)** Comparison of crosslinking patterns to Sec61 versus Sec61S353C with cysteine- and NH<sub>2</sub>-reactive SMPH. 17 eq microsomes per lane were crosslinked with 1 mM SMPH on ice for 30 min and proteins resolved by SDS-PAGE. Sec61 was detected with an antibody against its N-terminus. Note that both Sec61 and Sec61S353C crosslink to Sss1. Additional crosslinked bands occurring in Sec61S353C samples are indicated by arrows in Sec61 panel. The largest product consists of Sec61S353C crosslinked to Sec63 (right panel). **C)** Sec61S353C crosslinking with SMPH (non-cleavable) or LC-SPDP (cleavable). Crosslinking was done as above and samples were resolved on SDS-PAGE without or with 200 mM DTT in the sample buffer as indicated. **D)** Crosslinking patterns to Sec61S353C after microsome extraction. Microsomes (17eq/lane) were extracted as indicated or mock-treated, crosslinked as above, and Sec61S353C and crosslinking products detected with an antibody against the Sec61 N-terminus. Note that crosslinks to Sec63 and Sss1 are sensitive to carbonate extraction. **E)** Crosslinking of His<sub>14</sub>-Sec61S353C microsomes with LC-SPDP. Crosslinking was done as above. Note that the N-terminal His<sub>14</sub>-tag did not affect crosslinking to Sec63 or Sss1 indicating no gross conformational alterations in the Sec complex. (\*) indicates non-specific band that occurred independently of crosslinking in the Sec61 blot.

## 48 Results and Discussion

49 To identify new luminal interaction partners of Sec61 we used a functional *sec61* mutant with  
50 a unique cysteine in its large luminal loop 7 (Fig. 1A) (*Kaiser and Römisch, 2015*). Using hetero-  
51 bifunctional non-cleavable (SMPH) or cleavable (LC-SPDP) crosslinkers with a cysteine-reactive group  
52 and a NH<sub>2</sub>-reactive group to crosslink yeast microsomes, as described in Materials & Methods, we  
53 found additional bands in the crosslinking patterns to Sec61S353C compared to wildtype Sec61  
54 - suggesting bound luminal interactors (Fig. 1B, C, arrows). Amongst those was Sec63, a well-  
55 characterized J-domain protein that contributes to both co- and posttranslational import into the  
56 ER and to ERAD (Fig. 1B) (*Brodsky et al., 1995; Servas and Römisch, 2013*). While pretreatment of  
57 microsomes with urea had no effect on the Sec61S353C-associated proteins (Fig. 1D, lanes 4-6),  
58 extraction of microsomes with sodium carbonate resulted in reduced crosslinking to Sss1 which  
59 is known to be partially carbonate-extractable (*Esnault et al., 1994*) and to Sec63 (Fig. 1D, lanes  
60 10-12). Our data suggest an interaction between the Sec63 luminal J-domain or N-terminus with  
61 Sec61 loop7.

62 For enrichment of Sec61-crosslinked proteins we tagged the N-termini of Sec61 and Sec61S353C  
63 with 14-His which had no effects on growth, expression levels, or tunicamycin-sensitivity and UPR  
64 induction (not shown), indicating no perturbation of ER proteostasis. Crosslinking patterns were not  
65 affected by the tagging (Fig. 1E). Sec61- and Sec61S353C-crosslinked proteins were purified from  
66 500 eq lysed microsomes on a nickel column and eluted with imidazole (Fig. 2A). Fractions 3-10  
67 of the eluates were pooled and proteins analyzed by mass spectrometry. Proteins were accepted  
68 as interactors if there was at least a 3-fold enrichment compared to the uncrosslinked sample  
69 (Fig. 2B). In total, we identified 353 proteins that were copurifying with Sec61 in the crosslinked  
70 samples (supplementary table to Fig. 2). While the enrichment pattern was sample- and crosslinker-  
71 dependent (supplementary table to Fig. 2), the absolute abundance of proteins in the ER did not  
72 affect interaction with Sec61 (Fig. 2C) suggesting that the interactions we detected were specific.  
73 We detected all subunits of the Sec complex in the ER membrane, SRP receptor, Snd3, and several  
74 subunits of oligosaccharyl transferase (supplementary table to Fig. 2) (*Aviram et al., 2016; Wang  
75 and Dobberstein, 1999*). In the same significance range we found a number of new interaction  
76 partners of Sec61 that were ERAD relevant: Asi3, Ubc6, Ubc7, Cue1, Ubx7, Ubp1, Rpt2, ER-membrane  
77 complex (EMC) subunits, and Mpd1, suggesting close physical contact of the Sec61 channel with  
78 ERAD machinery (*Foresti et al., 2014; Römisch, 2005; Vembar and Brodsky, 2008; Ng et al., 2007;  
79 Baker et al., 1992; Christianson et al., 2011; Grubb et al., 2012*).

80 We then decided to investigate the interaction of Sec61 with Mpd1, a known ERAD factor of  
81 the well-characterized ERAD substrate CPY\* (*Grubb et al., 2012*). Our xQuest/xProphet analysis of  
82 crosslinked peptides suggested a direct interaction of Mpd1 C59 with K209 in luminal loop5 of  
83 Sec61 which constitutes the hinge region around which the N-terminal half of Sec61 swings during  
84 channel opening (Fig. 3A, upper) (*Leitner et al., 2014; Voorhees and Hegde, 2016*). Comparison of  
85 Sec61 loop5 with SecY loop5 of bacteria and archaea revealed a substantial extension of loop5  
86 in eukaryotes including the crosslinking site of Mpd1 (Fig. 3A, middle & lower). We hypothesized  
87 that the eukaryotic extensions in loop5 might serve as docking sites for ERAD factors to facilitate  
88 opening of the Sec61 channel from the lumen for export of ERAD substrates. To test this hypothesis  
89 we deleted sections of the Sec61 hinge including the Mpd1 contact site to create a smaller vestigial  
90 hinge within Sec61, similar to the SecY counterpart (Fig. 3A, middle & lower), and investigated  
91 the effects on protein transport into the ER and ERAD. While deletion1 caused temperature- and  
92 cold-sensitivity alone and in combination with deletion2 (Fig. 3B), steady-state expression levels of  
93 all hinge mutants were like wildtype (Fig. 4F), and there was no effect on co- or posttranslational  
94 protein import into the ER (Fig. 3C).



95

**Figure 2. Purification and proteomics of Sec61-crosslinked proteins. A)** 500 eq microsomes treated either with DMSO (control), SMPH (cleavable), or LC-SPDP (non-cleavable) were used. Samples were quenched and solubilized in IP Buffer. After denaturation (10 min, 65°C), proteins were diluted with cold Binding Buffer and applied to a HisTrap FF crude 1ml column. Fractionation was done using an imidazole gradient (100-500 mM). Sec61 and Sec63 were detected in each fraction after cleavage (LC-SPDP) and gel electrophoresis by immunoblotting with specific antibodies. **B)** Volcano plots based on the statistically determined protein enrichment in the crosslinked samples (His<sub>14</sub>-Sec61 and His<sub>14</sub>-Sec61S353C) when compared to the non-crosslinked samples. The horizontal axis represents log<sub>2</sub> fold change (log<sub>2</sub>FC) reflecting level of enrichment. The vertical axis plots the -Log<sub>10</sub>(pValue) of enrichment, reflecting significance. Both hits and candidates have a fold change of at least 3. Hits have a false discovery rate (FDR) < 5 % and candidates an FDR < 20 %. Purple line is at fold-change of 3. Hits shown as colored dots and candidates as triangles. Elements of Sec61 complex in green; known interactors or translation machinery in blue; and shortlisted hits in red and points labeled on graph. Not significant hits below reference line and non-interesting hits above reference line in light grey. **C)** Graphical representation of the enrichment level (i.e log<sub>2</sub>FC) of the Sec61 interactors as function of their respective cellular abundance as in *Kulak et al. (2014)*. Known interactors blue, Sec61 complex subunits green, interesting interactors red and labeled on the graph. Note absence of correlation between cellular abundance and interaction with Sec61. **Figure 2 - Figure supplement 1** Table with mass spectrometry statistical analysis (hit and candidate determination).

96

As only the double mutant *sec61del1/2* showed a moderate tunicamycin-sensitivity (Fig. 3B) and slightly induced UPR (Fig. 3 - Figure supplement 1), ER-proteostasis was not dramatically compromised in the mutants excluding gross ERAD defects. This was confirmed by normal ERAD kinetics for the KHN, KWW, and pΔgpαF substrates in the mutants (Fig. 4A,B,C) (Pilon *et al.*, 1997; Vashist and Ng, 2004). CPY\* degradation, however, was compromised in *sec61del1* which lacks the contact site for Mpd1 (Fig. 4D, magenta). In contrast, *sec61del2* barely affected CPY\* degradation (Fig. 4D, red). The *sec61del1/2* mutant had an intermediate phenotype (Fig. 4D, green) which may suggest that it was not just the absence of specific amino acids deleted in *sec61del1*, but also the distortion of the hinge by the deletion that caused the CPY\* ERAD defect (Fig. 3A, lower). In *sec61del1/2* this distortion is partially compensated (Fig 3A, lower).

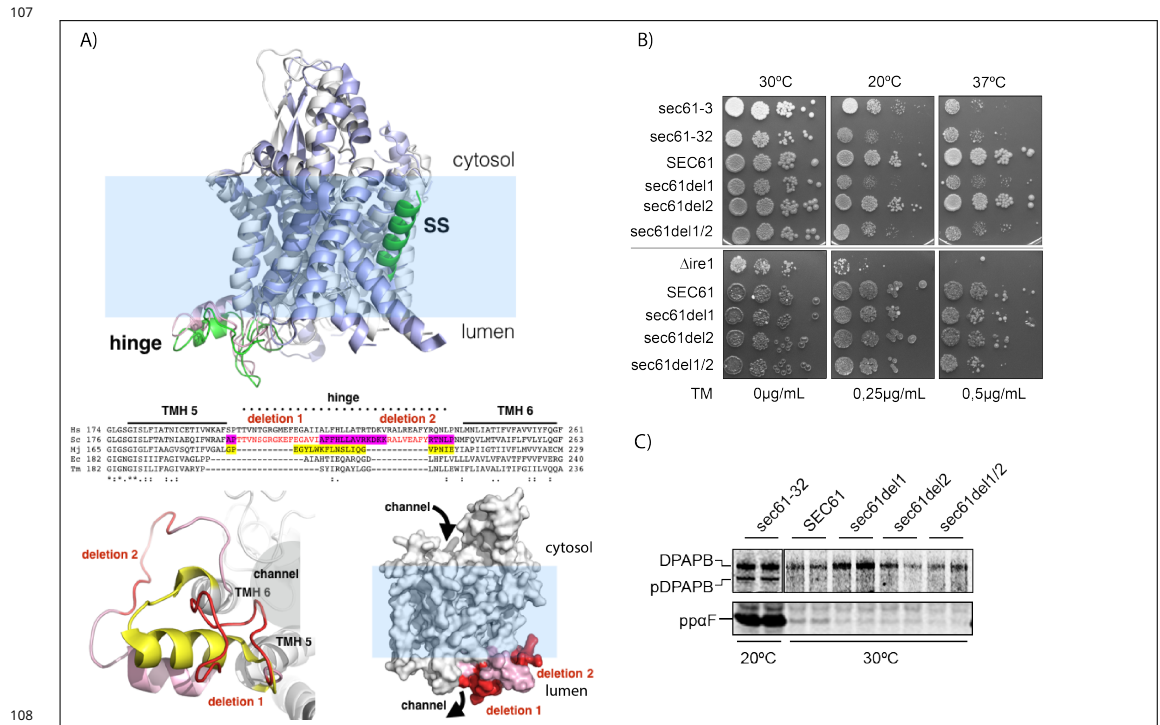


**Figure 3. Design and characterization of *sec61* loop5 hinge mutants encompassing the binding site for Mpd1. A)** Top: Structure of the Sec61 channel in closed (grey helices, pink hinge) versus open state (blue helices, green hinge, green signal sequence (SS) inserted in lateral gate) (Voorhees and Hegde, 2016) (PDB 3J7Q, PDB 3J7R). Note conformational changes in hinge (pink vs green) during channel opening. Middle: Alignment of loop5 hinge sequences of eukaryotes (*Homo sapiens*, Hs; *Saccharomyces cerevisiae*, Sc), prokaryotes (*Escherichia coli*, Ec; *Thermotoga maritima*, Tm) and archaea (*Methanococcus jannaschii*). Protein sequences were obtained from Uniprot. Regions coded by deletions in our *sec61* mutants are shown in red. The sequence forming the archaeal hinge region is highlighted in yellow, and the sequence corresponding to the vestigial (post-deletion) eukaryotic counterpart is highlighted in magenta. Bottom left: view of the hinge from the ER lumen (eukaryotic - PDB 3J7Q), showing the protein channel lined by TMHs 5, along with 6 and the intervening hinge (pink) with deletions 1 and 2 in red. The deletions result a shorter hinge akin to the archaeal structure shown in yellow (PDB 1RHZ) (also see middle). Bottom right: space filling model of Sec61 channel (PDB 3J7Q) in ER membrane indicating positions of deletions 1 and 2. Note that the region deleted in *sec61del1* is accessible for luminal proteins in contrast to *sec61del2* which faces the membrane (lower right). **B)** Growth of *SEC61* and *sec61* hinge deletion mutants at different temperatures (30°C, 20°C, 37°C; top) or in the presence of tunicamycin (TM - 0 g/ml, 0.25 g/ml, 0.5 g/ml; all grown at 30°C, bottom). Cells ( $10^4$  to  $10^6$ ) were grown on YPD plates for 3 days. The following strains were used as controls: *sec61-32*, *sec61-32*, and *Δire1*. **C)** Analysis of ER import in *sec61* hinge mutants. Early log-phase cells were pulse labeled with [ $^{35}$ S]-met/cys, lysed, and DPAPB (upper; cotranslational import) or prepro alpha-factor (ppαF) (lower; posttranslational import) immunoprecipitated. Starving and labeling were done at 30°C for all strains, except for *sec61-32*, which was incubated at 20°C. Labelling was done for 5 min for ppαF and 15 min for DPAPB. Proteins were detected by phosphorimaging. **Figure 3 - Figure supplement 1. HAC1 mRNA Splicing Assay to evaluate UPR induction in *sec61* hinge mutants.**

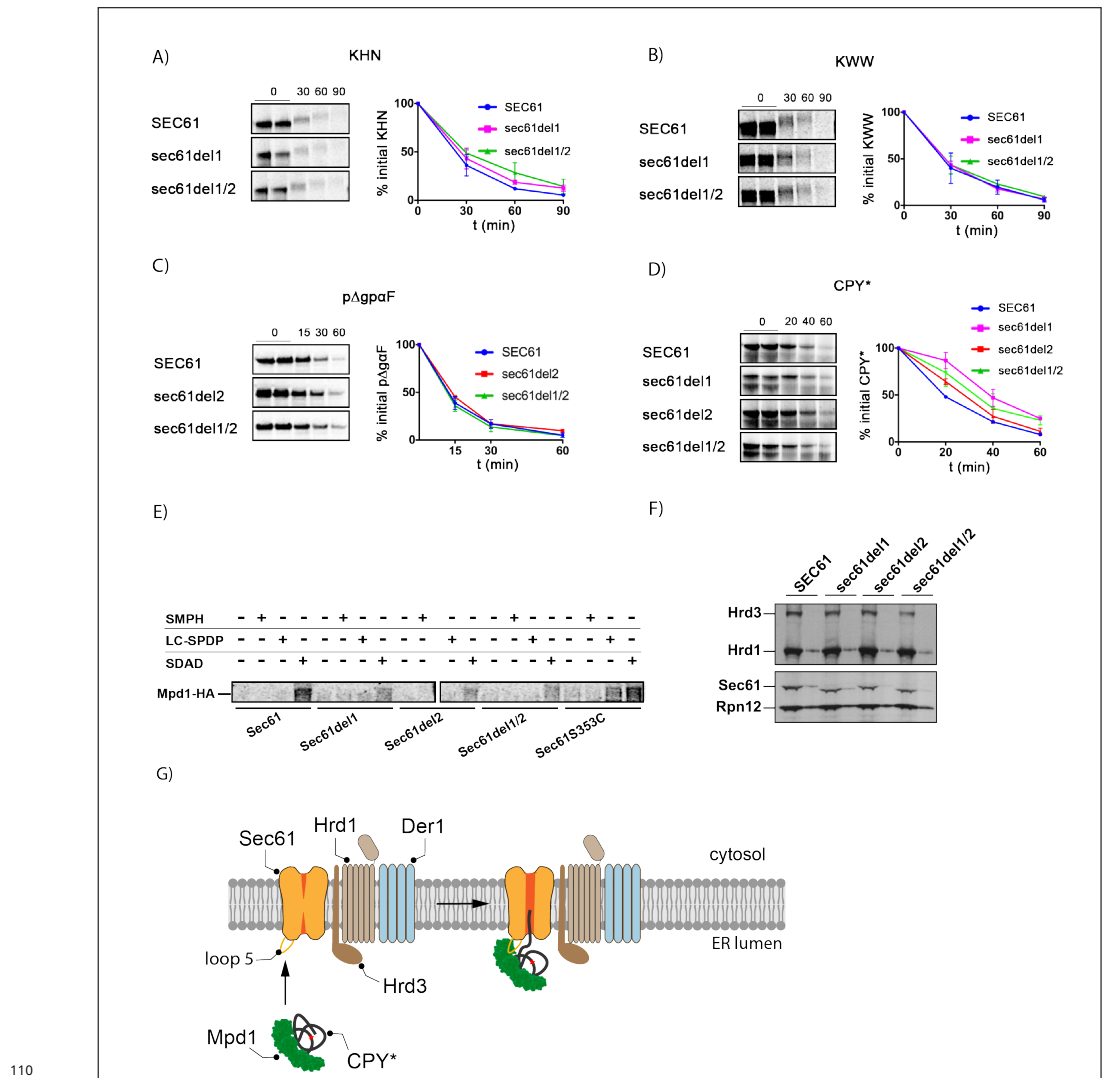


**Figure 4. Mutation of the loop5 hinge in Sec61 specifically affects CPY\* ERAD and interaction with Mpd1.** **A) - D)** The *sec61* hinge mutants were screened for ERAD defects for: KWN; KWW, pAgpaF, and CPY\*. Wildtype and mutant strains were pulse-labeled with [<sup>35</sup>S]-met/cys for 5 (pAgpaF and CPY\*) or 15 min (KWW and KWN) followed by chase incubations for the indicated times. For each time point 1.5 OD<sub>600</sub> of cells were lysed and proteins immunoprecipitated using specific antibodies (CPY\*, pAgpaF) or anti-HA. After SDS-PAGE, proteins were detected by phosphorimaging. Bands were quantified using ImageQuant (GE Healthcare) and averaged values plotted. For each experiment, at least three replicas were made. **E)** Interaction of Sec61 with Mpd1 was determined by crosslinking in [<sup>35</sup>S]-met/cys-labeled microsomes treated with SMPH (cysteine and NH<sub>2</sub>-reactive, non-cleavable), LC-SPDP (cysteine and NH<sub>2</sub>-reactive, cleavable) or SDAD (NH<sub>2</sub>-reactive and photoactivatable, cleavable) as indicated. For explanations of the crosslinker selection, see Material & Methods. Sec61 and crosslinked proteins were precipitated with anti-Sec61 N-terminal antibodies, followed by reduction of the crosslinker. Subsequently, Mpd1-HA was precipitated using HA-antibodies. After gel electrophoresis, proteins were detected by phosphorimaging. Equal amounts of cells were used for the preparation of each microsome batch. Protein levels of both Sec61 and Mpd1-HA were similar in all strains. Saturating amounts of antibodies were used for each precipitation. **F)** Steady state level of Sec61, Hrd1, and Hrd3 were determined by immunoblotting in wildtype and *sec61* hinge mutants. Two different amounts of cell lysates (1 and 1/3) of each sample were loaded side by side. Rpn12 was used as loading control. Specific antibodies for the different proteins were used for immunoblotting. **G)** Model for initiation of CPY\* ERAD mediated by Mpd1 interaction with Sec61.

To directly confirm that the Mpd1 interaction with Sec61 was compromised in the *sec61* hinge mutants we prepared radiolabelled microsomes from wildtype, *sec61S353C* and *sec61* hinge mutant strains expressing HA-tagged Mpd1 and performed sequential immunoprecipitations with Sec61

115 and HA-antibodies. In all hinge mutants less Mpd1 was associated with Sec61 compared to wildtype  
 116 or Sec61S353C (Fig. 4E), but it was not possible to correlate that amount of Mpd1 bound to  
 117 mutant Sec61 with the degree of the CPY\* ERAD defect (compare Figs. 4D, 4E). To exclude that the  
 118 *sec61* hinge mutants reduced biogenesis of the ER ubiquitin ligase Hrd1 and its cofactor Hrd3 we  
 119 performed quantitative immunoblots for both proteins and found that they were expressed equally  
 120 in wildtype and mutant cells (Fig. 4F).

121 Collectively, our data suggest that interaction of the CPY\* ERAD factor Mpd1 with the Sec61  
 122 hinge region in loop5 contributes to export and degradation of this substrate. Our results are  
 123 consistent with the view that Sec61 forms part of an export complex in the ER membrane for  
 124 misfolded protein transport to the cytosol (Fig. 4G). The extended hinge in Sec61 compared to  
 125 SecY (Fig. 3A) may serve to activate and open the channel for the lumen for intercalation and  
 126 subsequent transport of CPY\* to the cytosol (Fig. 4G).

## 127 Materials and Methods

128 *S. cerevisiae* strains used in this study are listed in **Table 1**, plasmids in **Table 2**, primers in **Table 3**,  
 129 and antibodies in **Table 4**

**Table 1.** *S. cerevisiae* strains used in this study.

Name	Genotype	Reference
KRY37	<i>MAT<math>\alpha</math> his4 trp1 leu2 ura3 HOL1-1 sec61-3</i>	<i>Stirling et al. (1992)</i>
KRY157	<i>Mata leu2 his3 trp1 ura3 ade2 sec61::HIS3 can1-100 [pDQ sec61-32]</i>	<i>Pilon et al. (1997)</i>
KRY160	<i>MAT<math>\alpha</math> leu2 his3 trp1 ura3 ade2 can1-100 leu2::LEU+UPRE-lacZ MET+ ire1::TRP1</i>	<i>Shamu and Walter (1996)</i>
KRY461	<i>MAT<math>\alpha</math> sec61::HIS3 leu2 trp1 prc1-1 his3 ura3 [pGAL-SEC61-URA3]</i>	<i>Tretter et al. (2013)</i>
KRY853	<i>MAT<math>\alpha</math> leu2 ura3 [pRS306-truncsec61-S353C]</i>	<i>Kaiser and Römisch (2015)</i>
KRY897	<i>MAT<math>\alpha</math> sec61::HIS3 leu2 trp1 prc1-1 his3 ura3 [pRS315-SEC61-LEU]</i>	<i>Tretter et al. (2013)</i>
KRY1061	<i>MAT<math>\alpha</math> sec61::HIS3 leu2 trp1 prc1-1 his3 ura3 [pRS315-pGal-14His-Sec61S353C-LEU]</i>	This work
KRY1081	<i>MAT<math>\alpha</math> sec61::HIS3 leu2 trp1 prc1-1 his3 ura3 [pRS315-pGal-14His-SEC61-LEU]</i>	This work
KRY1116	<i>MAT<math>\alpha</math> sec61::HIS3 leu2 trp1 prc1-1 his3 ura3 [pRS315-sec61del1-LEU]</i>	This work
KRY1117	<i>MAT<math>\alpha</math> sec61::HIS3 leu2 trp1 prc1-1 his3 ura3 [pRS315-sec61del2-LEU]</i>	This work
KRY1118	<i>MAT<math>\alpha</math> sec61::HIS3 leu2 trp1 prc1-1 his3 ura3 [pRS315-sec61del1/2-LEU]</i>	This work
KRY1162	<i>MAT<math>\alpha</math> sec61::HIS3 leu2 trp1 prc1-1 his3 ura3 [pRS315-SEC61-LEU] [pRS426-MPD1-HA-URA]</i>	This work
KRY1163	<i>MAT<math>\alpha</math> sec61::HIS3 leu2 trp1 prc1-1 his3 ura3 [pRS315-sec61del1-LEU] [pRS426-MPD1-HA-URA]</i>	This work
KRY1164	<i>MAT<math>\alpha</math> sec61::HIS3 leu2 trp1 prc1-1 his3 ura3 [pRS315-sec61del2-LEU] [pRS426-MPD1-HA-URA]</i>	This work
KRY1165	<i>MAT<math>\alpha</math> sec61::HIS3 leu2 trp1 prc1-1 his3 ura3 [pRS315-sec61del1/2-LEU] [pRS426-MPD1-HA-URA]</i>	This work

**Table 2.** Plasmids used in this study.

Name	Description	Reference
pBW11	<i>SEC61</i> in pRS315	<i>Tretter et al. (2013)</i>
pRS315	CEN vector ( <i>LEU2</i> )	<i>Sikorski and Hieter (1989)</i>
pRS426	2 $\mu$ vector ( <i>URA3</i> )	<i>Kaiser and Römisch (2015)</i>
pRS315- <i>sec61S353C</i>	<i>sec61S353C</i> in pRS315	
pRS315-His <sub>14</sub> - <i>sec61S353C</i>	<i>GAL1-His<sub>14</sub>-sec61S353C</i> in pRS315	This work
pRS315-His <sub>14</sub> - <i>SEC61</i>	<i>GAL1-His<sub>14</sub>-SEC61</i> in pRS315	This work
pRS315- <i>sec61del1</i>	<i>sec61del1</i> in pRS315	This work
pRS315- <i>sec61del2</i>	<i>sec61del1</i> in pRS315	This work
pRS315- <i>sec61del1/2</i>	<i>sec61del1/2</i> in pRS315	This work
pRS426GAL1	pGAL1+ N-terminal His <sub>14</sub> -tag	<i>Stein et al. (2014)</i>
p416p $\Delta$ <i>gpaF</i>	overexpression of p $\Delta$ <i>gpaF</i> ( <i>URA3</i> ), contains MET25 promoter	<i>Gillece et al. (1999)</i>
pSM101	<i>KWW-HA (URA3)</i>	<i>Vashist and Ng (2004)</i>
pSM70	<i>KHN-HA (URA3)</i>	<i>Vashist and Ng (2004)</i>
pYM24	hphNT1 marker with 3xHA tag	<i>Janke et al. (2004)</i>

**Table 3.** Primers used in this study.

Name	Sequence (5' → 3')	Restriction Site	Application
Primer 1	ATGTCCTCCAACCGTGT	-	His <sub>14</sub> tagging
Primer 2	CAACTTCCTAAGCTTCACGCC	HindIII	His <sub>14</sub> tagging
Primer 3	GCTGGAGCTCTAGTACG	SacI	His <sub>14</sub> tagged subcloning
Primer 4	GCAAATTAAGCCTTCGA	-	His <sub>14</sub> tagged subcloning
Primer 5	AAGCTTAAGCTTGCTATAAGCTA GAATGTATTGAATGTATTC	-	Loop 5 SOE
Primer 6	GGATCCGCGCATTGCTTAAGC AAG- GATACC	HindIII	Loop 5 SOE
Primer 7	GGAAAAAGGCAGGAGCAAACG CTCTCCAG	BamHI	Loop 5 SOE
Primer 8	CGTTTGCTCCTGCCTTTTCCCA TCTTTTGCTG	-	Loop 5 SOE
Primer 9	GGACAAGAAATACCGTACCAA TCTACCTAATATGTTCC	-	Loop 5 SOE
Primer 10	TGGTACGGTATTTCTTGTCCT TTCT- GACAGCC	-	Loop 5 SOE
Primer 11	CCTTTGTCGACTAGTGTCATGTG	SpeI	<i>MPD1</i> HA tagging
Primer 12	GCAGCGAGGTACCGTAATTTTTC	KpnI	<i>MPD1</i> HA tagging
Primer 13	GGATACAAGTCGACGCAAATTTCTC	Sall	<i>MPD1-HA</i> subcloning
Primer 14	CAATTTTGGATGGGAATTCAATTATAC	EcoRI	<i>MPD1-HA</i> subcloning



**Table 4.** *S. cerevisiae* strains used in this study.

Name	Source	Dilution
Anti-Sec61(N-terminus)	KB Römisch	Western Blot 1: 2.500; IP 1:100
Anti-Sec61(C-terminus)	KB Römisch	Western Blot 1: 2.500; IP 1:100
Anti-Sec63	Schekman lab	Western Blot 1:2.500; IP 1:100
Anti-Rpn12	Römisch lab	Western Blot 1:2.500
Anti-Hrd1	T. Sommer lab	Western Blot 1:10.000
Anti-Hrd3	T. Sommer lab	Western Blot 1:10.000
Anti-HA	BioLegend	Western Blot 1:5.000 ; IP 1:200
Anti-CPY	KB Römisch lab	IP 1:100
Anti-ppaF	KB Römisch lab	IP 1:100
Anti-DPAPB	Stevens lab	IP 1:100
Anti- rabbit (HRP)	Rockland™	Western Blot 1:10.000

### 130 **Growth of *S. cerevisiae***

131 *S. cerevisiae* cells were grown at 30°C in YPD or in SC medium with continuous shaking at 220  
132 rpm. Cells on solid medium were also grown at 30°C if not stated otherwise. To test temperature  
133 sensitivity, cells were counted and serial dilutions were prepared. A volume of 5 µl of each dilution  
134 (containing 10<sup>4</sup> – 10 cells) was pipetted onto YPD plates. To test tunicamycin (Tm) (SIGMA) sensitivity,  
135 cells were grown on YPD plates supplemented with 0, 0.25 or 0.5µg/ml Tm. Plates were incubated  
136 at indicated temperatures for 3 days.

### 137 **Yeast Microsome Preparation**

138 The isolation of rough microsomal membranes from *S. cerevisiae* was done as in *Pilon et al. (1997)*  
139 and membranes aliquoted at an  $OD_{280}=30$ , snap-frozen in liquid nitrogen, and stored at -80°C.  
140 Microsome amounts are referred to as equivalents (eq) in which 1 eq = 1 µl of microsomes at an  
141  $OD_{280}$  of 50 (*Walter et al., 1981*).

142 To prepare radiolabeled ER vesicles, 7  $OD_{600}$  of early log-phase cells were incubated in synthetic  
143 minimal media supplemented appropriately and lacking methionine, cysteine, and ammonium  
144 sulfate for 30 min at 30°C, 220 rpm. Cells were labelled with 6,5 MBq [35S] methionine/cysteine  
145 (Express Labeling, PerkinElmer) mix for 30 min. After labelling, cells were immediately washed twice  
146 with Tris-Azide Buffer (20 mM Tris-HCl, pH 7.5, 20 mM sodium azide). Cells were then incubated in  
147 100 mM Tris-HCl, pH 9, 10 mM DTT for 10 min at room temperature, sedimented, and resuspended  
148 in 300 µl of 2 x JR Lysis Buffer (40 mM Hepes-KOH, pH 7.4 , 400 mM sorbitol, 100 mM KOAc, 4  
149 mM EDTA, 1 mM DTT, 1 mM PMSF) (*Pilon et al., 1997*). Acid-washed glass beads (1/2 volume) were  
150 added and the sample submitted at 2 cycles of 1 min bead-beating (Mini-beadbeater-16, BioSpec)  
151 with 2 min of incubation on ice after each cycle. From this point on, all samples were kept at  
152 4°C. Beads were washed 3 times with 300 µl of B88, pH 7.2 (20 mM Hepes-KOH pH 6.8, 250 mM  
153 sorbitol, 150 mM KOAc, 5 mM Mg(OAc)<sub>2</sub>). Washes were pooled and sedimented for 2 min at 1,500 x  
154 g and the microsome-containing supernatant was transferred to a clean tube. Microsomes were  
155 then sedimented at 16,000 x g for 10 min, washed and resuspended in 200 µl B88, pH 7.2. Crude  
156 radiolabelled ER vesicles were then aliquoted (50 µl), flash frozen in liquid nitrogen, and stored at  
157 -80°C.

### 158 **Chemical Crosslinking**

159 Microsomes (17 eq) were washed and resuspended in B88 (20 mM Hepes-KOH, 250 mM sorbitol, 150  
160 mM KOAc, 5 mM Mg(OAc)<sub>2</sub>). For SMPH and LC-SPDP crosslinking B88 was used at pH 7.2, for SDAD  
161 crosslinking pH was 7.9. The total reaction volume for subsequent detection by immunoblotting  
162 was 100 µl with appropriate amount of crosslinker (SMPH or LC-SPDP: 1 mM; SDAD: 1.5 mM).

163 Control reactions were prepared with 5  $\mu$ l of DMSO, but otherwise treated identically. For up-scaling,  
164 proportion of microsomes/total volume was maintained. After crosslinker addition, samples were  
165 incubated on ice for 30 min. Then, Quenching Buffer (1M Tris-HCl, pH 8; 100 mg/ml L-cys) was  
166 added (1/10 of total volume), and the sample incubated on ice for 15 min. Samples were then  
167 washed twice (always in the presence of quenching buffer) with appropriate pH B88, membranes  
168 sedimented at 16,000 x g for 10 min, and resuspended in appropriate form for subsequent use. For  
169 LC-SPDP cleavage, membranes were incubated for 15 min at room temperature in the presence of  
170 100 mM of DTT. For SDAD crosslinking, after the washes the sample was exposed, on ice, to a 15  
171 min UV (365 nm) irradiation with a 3UV Lamp (115V, 60Hz) (ThermoFisher) at a distance of 3,6 cm.

### 172 **Extraction of Luminal and Cytosolic Microsome-Associated Proteins**

173 For extraction of cytosolic membrane-associated proteins, microsomes were resuspended in  
174 B88/Urea (20 mM Hepes-KOH, pH 6.8, 250 mM sorbitol, 150 mM KOAc, 5 mM Mg(OAc)<sub>2</sub>, 2,5  
175 M urea), incubated for 20 min on ice, followed by sedimentation and washing of the membranes  
176 with B88, pH 6.8. For extraction of ER-luminal proteins, microsomes were resuspended in 100 mM  
177 sodium carbonate, pH 11.5, incubated on ice for 20 min, followed by sedimentation (20 min at  
178 346,000xg, 4°C) of the membranes through a sucrose cushion (200 mM sucrose, 100 mM sodium  
179 carbonate, pH 11.5), and resuspension in B88, pH 6.8. For mock extractions, samples were treated  
180 in same way, but in absence of either urea or sodium carbonate.

### 181 **Immunoblotting**

182 Protein gel electrophoresis was conducted using NuPAGE Novex pre-cast Bis-Tris gels (4–12,5% gels,  
183 1.0 mm) and the XCell SureLock Mini-Cell (both Invitrogen). Proteins were transferred to nitrocellu-  
184 lose membranes (BioRad) and detected with specific antibodies at the appropriate dilutions, and an  
185 ECL reagent (Pierce) according to the supplier's instructions. Signal was acquired either using an  
186 Amersham Imager 600 (GE Healthcare) or exposure to ECL films (Adavnstta).

### 187 **Purification of Sec61**

188 ER membranes (500 eq) were treated as described in "Chemical Crosslinking", either with DMSO  
189 (control), SMPH, or LC-SPDP in a total volume of 1.5 ml. After washing, membranes were resus-  
190 pended in 150  $\mu$ l of Quenching Buffer (1 M Tris-HCl, pH 8; 100 mg/ml L-cys) and diluted with 1 ml  
191 of IP Buffer (15 mM Tris-HCl, pH 7.5, 150 mM NaCl, 1 % Triton X-100, 0,1 % SDS) for solubilization  
192 (30 min at 4°C) followed by 10 min denaturation at 65°C. From this point on, all steps were done  
193 at 4°C. Sample was diluted with cold Binding Buffer (50 mM Tris-HCl, 300 mM KCl, 0,5 % Triton X-  
194 100, 40 mM imidazole) to a final volume of 5 ml and applied to an HisTrap FF crude (1 ml) column  
195 integrated into a BioLogic automated purification system (Biorad). After sample loading (0.5 ml/min  
196 for 10 ml), the column was washed with Binding Buffer (10 ml; 1 ml/min) and sample eluted along  
197 a step gradient of imidazole (100-500 mM, 15 ml per step, 1ml/min. Steps: 100; 200; 400; 500).  
198 Fractions (7,5 ml) were collected along the gradient with an automatic fraction collector. DTT (100  
199 mM) was added to each fraction. Each differently treated sample was applied to an independent  
200 column. Between purifications, the system was washed with 10 ml H<sub>2</sub>O, 10 ml ethanol 20 %, 10  
201 ml H<sub>2</sub>O, 20 ml Binding Buffer. Fractions where Sec61 was eluted (fraction 3-10 - 50 ml total) were  
202 pooled, proteins precipitated with 10 % TCA on ice for 2h and washed with ice-cold acetone. Each  
203 pellet was resuspended in 2 x Laemmli Buffer, and resolved for 5 cm on 4-12,5% NuPAGE gel. The  
204 gel was then stained by Coomassie Colloidal Staining (0.08% Coomassie Brilliant Blue G250 (CBB  
205 G250), 10 % citric acid, 8% ammonium sulfate, 20 % methanol) overnight and destained with water  
206 as described in the EMBL online Proteomics Core Facility Protocols. The gels where then sealed in  
207 individual plastic bags with a few milliliters of water and shipped to the Mass Spectrometry Facility.

## 208 **Mass Spectrometry**

### 209 Sample preparation

210 The whole lane of each samples was cut out into small cubes and subjected to in-gel digestion  
211 with trypsin (*Savitski et al., 2014*). After overnight digestion, peptides were extracted from the gel  
212 pieces by sonication for 15 minutes, tubes were centrifuged, the supernatant removed and placed  
213 in a clean tube. Followed by a second extraction round with a solution of 50:50 water: acetonitrile,  
214 1% formic acid (2 x the volume of the gel pieces) and the samples were sonicated for 15 minutes,  
215 centrifuged and the supernatant pooled with the first extract. The pooled supernatants were then  
216 subjected to speed vacuum centrifugation. Samples were reconstituted in 96:4 water: acetonitrile,  
217 0.1% formic acid and further processed using an OASIS® HLB  $\mu$ Elution Plate (Waters) according to the  
218 manufacturer's instructions.

### 219 LC-MS/MS

220 Peptides were separated using the nanoAcquity Ultra Performance Liquid Chromatography (UPLC)  
221 system (Waters) using a trapping (nanoAcquity Symmetry C18, 5  $\mu$ m, 180  $\mu$ m x 20 mm) as well as  
222 an analytical column (nanoAcquity BEH C18, 1.7  $\mu$ m, 75  $\mu$ m x 200 mm). The outlet of the analytical  
223 column was coupled to a Linear Trap Quadrupole (LTQ) Orbitrap Velos Pro (Thermo Fisher Scientific)  
224 using the Proxeon nanospray source. Solvent A consisted of water, 0.1% formic acid and solvent  
225 B consisted of acetonitrile, 0.1% formic acid. Sample was loaded with a constant flow of solvent  
226 A at 5  $\mu$ l/min onto the trapping column. Peptides were eluted over the analytical column with a  
227 constant flow of 0.3  $\mu$ l/min During elution the percentage of solvent B increased linearly from 3% to  
228 7% in 10 min., then increased to 25% in 110 min and to 40% for the final 10 min a cleaning step  
229 was applied for 5 min with 85% B followed by 3% B 20 min. The peptides were introduced into  
230 the mass spectrometer via a Pico-Tip Emitter 360  $\mu$ m OD x 20  $\mu$ m ID; 10  $\mu$ m tip (New Objective),  
231 a spray voltage of 2.2 kV was applied. Capillary temperature was 300 °C. Full scan MS spectra  
232 were acquired with a resolution of 30000. The filling time was set at a maximum of 500 ms with a  
233 maximum ion target of  $1.0 \times 10^6$ . The fifteen most intense ions from the full scan MS (MS1) were  
234 sequentially selected for sequencing in the LTQ. Normalized collision energy of 40% was used, and  
235 the fragmentation was performed after accumulation of  $3.0 \times 10^4$  ions or after a maximum filling  
236 time of 100 ms for each precursor ion (whichever occurred first). Only multiply charged (2+, 3+, 4+)  
237 precursor ions were selected for MS/MS. The dynamic exclusion list was restricted to 500 entries  
238 with maximum retention period of 30 s and a relative mass window of 10 ppm. In order to improve  
239 the mass accuracy, a lock mass correction using the ion (m/z 445.12003) was applied.

### 240 Data analysis

241 The raw mass spectrometry data was processed with MaxQuant (v1.5.2.8) (*Cox and Mann, 2008*) and  
242 searched against an Uniprot *Saccharomyces cerevisiae* proteome database. The search parameters  
243 were as follows: Carbamidomethyl (C) (fixed), Acetyl (N-term) and Oxidation (M) (variable) were used  
244 as modifications. For the full scan MS spectra (MS1) the mass error tolerance was set to 20 ppm,  
245 and for the MS/MS spectra (MS2) to 0.5 Da. Trypsin was selected as protease with a maximum of  
246 two missed cleavages. For protein identification a minimum of one unique peptide with a peptide  
247 length of at least seven amino acids and a false discovery rate below 0.01 were required on the  
248 peptide and protein level. The match between runs function was enabled, a time window of one  
249 minute was set. Label free quantification was selected using iBAQ (calculated as the sum of the  
250 intensities of the identified peptides and divided by the number of observable peptides of a protein)  
251 (*Schwanhäusser et al., 2011*) with the log fit function enabled.

252 We also used the xQuest/xProphet pipeline (*Leitner et al., 2014*) to identify crosslinked peptides  
253 in our samples. For this, we used the basic protocol and conditions used in *Leitner et al. (2014)*,  
254 correcting the meaningful parameters to fit our crosslinker (e.g monoisotopic shift, only light chain,  
255 reactive groups, etc.). Databases of no more than 30 proteins were fed into the pipeline.

## 256 Statistical Analysis

257 The raw output data of MaxQuant (proteinGroups.txt file) was processed using the R programming  
258 language (ISBN 3-900051-07-0). As a quality filter we allowed only proteins that were quantified with  
259 at least 2 unique peptides. Potential batch-effects were removed from the log<sub>2</sub> of the iBAQ values  
260 using the limma package (*Ritchie et al., 2015*). Furthermore, batchcleaned data were normalized  
261 with the vsn package (variance stabilization) (*Huber et al., 2002*). Missing values were imputed using  
262 the MSNbase package (*Gatto and Lilley, 2012*). For conditions with at least 2 out of 3 identifications,  
263 the “knn” method was used. For less identifications, the “MinDet” method was applied. Finally,  
264 limma was used again to identify differentially expressed proteins. A protein was called a hit with  
265 a false discovery rate (fdr) smaller 5 % and a fold change of at least 3 and a candidate with a fdr  
266 smaller 20 % and a fold change of at least 3.

## 267 Mutant Construction

### 268 14His-Tagged constructs

269 For His<sub>14</sub>-tagging of *SEC61* and *sec61S353C*, both genes were amplified from pBW11 and pRS315-  
270 *sec61S353C*, respectively, using Primer 1 and Primer 2. The resulting PCR products were cloned into  
271 pRS426pGAL1 (*Stein et al., 2014*) using the SfoI and HindIII restriction sites. Correct cloning was  
272 confirmed by sequencing. The pGal-His<sub>14</sub>-*SEC61*-CYC and pGal-His<sub>14</sub>-*Sec61S353C*-CYC cassettes were  
273 then amplified using Primer 3 and Primer 4. The resulting PCR products were cloned into pRS315  
274 (CEN, LEU2). Transformants in the JDY638 (pGAL-*SEC61*-URA3) *S. cerevisiae* background were first  
275 selected on SC -URA medium containing 2% (w/v) galactose and 0.2% (w/v) glucose lacking leucine.  
276 The pGAL-*SEC61* plasmid was selected against on SC 5-FOA plates containing 2% (w/v) galactose  
277 and 0.2% (w/v) glucose without leucine. Constructs were confirmed by sequencing.

### 278 *SEC61* Loop 5 deletion mutants

279 Mutants *sec61del1*, *sec61del2*, and *sec61del1/2* were generated by PCR-driven overlap extension  
280 (SOE PCR) (*Aiyar et al., 1996; Horton et al., 1989*) followed by transformation into KRY461 of the  
281 respective constructs. For the initial SOE-PCR reactions, *SEC61* was amplified from pBW11 (Table 2).  
282 Deletion 1 and deletion 2 were made separately. Deletion 1/2 was made using deletion 1 construct  
283 as template and same primers as used for the generation of deletion 2. For SOE-PCR, the regions  
284 upstream and the downstream of the deletion sites were amplified using a mutagenic primer and a  
285 gene flanking primer (Table 3). Each mutagenic primer immediately flanks the deletion site and  
286 both upstream and downstream deletion-flanking primer have a stretch of complementarity with  
287 each other. For the extension of the final PCR product, the gene-flanking primer-pair was used and  
288 both upstream and downstream fragments were used as template (working as a single-template  
289 unit). The resulting PCR products were cloned into pRS315 (CEN, LEU2) (*Sikorski and Hieter, 1989*).  
290 Transformants into JDY638 (pGAL-*SEC61*-URA3) were first selected on SC -URA medium containing  
291 2% (w/v) galactose and 0.2% (w/v) glucose without leucine. The pGal-*SEC61* plasmid shuffle was  
292 done on SC 5'-FOA plates lacking leucine. All constructs were confirmed by sequencing.

### 293 *MPD1* HA-Tagging

294 Tagging of genomic *MPD1* was done as described in *Janke et al. (2004)*. Briefly, the HA cassette  
295 was amplified from pYM24 (supplied by Michael Knop) using Primer11 and Primer12. The plasmid  
296 contains the HA-cassette as well as the hphNT1 for selection. Targeting was done by homology of the  
297 designed primers with the appropriate regions of the gene of interest. This PCR product was then  
298 used to transform KRY461, and transformants were selected on YPD plates containing hygromycin  
299 (300µg/ml). *MPD1-HA* was amplified from the genomic DNA using Primer13 and Primer14 and  
300 cloned into pRS426 (2µM, URA3). This plasmid was then used to transform the hinge mutant strains.

## 301 Cell Labelling and Immunoprecipitation

302 Aliquots of 1.5 OD<sub>600</sub> early log phase cells were incubated in synthetic media lacking methionine,  
303 cysteine, and ammonium sulfate for 15 or 30 min (depending on the protein to be labelled) at the

304 appropriate temperature and shaking at 220 rpm. Cells were labeled with [<sup>35</sup>S]-met/cys (Express  
305 Labeling, PerkinElmer) (1.5 MBq per sample) mix for 5 min (CPY\*, pΔgpαF) or 15 min (DPAPB, KWW,  
306 KHN). For pulse experiments, after labeling cells were immediately killed with Tris-Azide Buffer (20  
307 mM Tris-HCl, pH 7.5, 20 mM sodium azide). For pulse-chase experiments, zero time points were  
308 treated as above, and to remaining samples Chase Mix (0.03% cys, 0.04% met, 10 mM ammonium  
309 sulfate) was added, and samples were incubated with shaking at the appropriate temperature for  
310 the indicated times. At each time point, Tris-Azide Buffer was added. Cells were harvested and  
311 incubated in 100 mM Tris-HCl, pH 9.4, for 10 min at room temperature. Subsequently, samples  
312 were lysed with glass beads in Lysis Buffer (20 mM Tris-HCl, pH 7.5, 2% (w/v) SDS, 1 mM DTT, 1  
313 mM PMSF) and denatured for 5 min at 95°C (soluble proteins) or 10 min at 65°C (transmembrane  
314 proteins). Afterwards, glass beads were washed 3 times and the combined washes used for  
315 immunoprecipitation after preclearing with 60 μl 20% Protein A-Sepharose beads (GE Healthcare)  
316 in IP-buffer (15 mM Tris-HCl, pH 7.5, 150mM NaCl, 1% Triton X-100, 0,1% SDS) (*Pilon et al., 1997*).  
317 Precipitations were done with 60 μl 20% Protein A-Sepharose beads (GE Healthcare) and appropriate  
318 amount of antibody, either at room temperature for 2h or at 4°C for 4h or over night. Protein  
319 A-Sepharose beads were washed as in Baker et al. (1988), proteins eluted with 2x Laemmli Buffer  
320 and denatured at 95°C for 5 min (soluble) or 65°C for 10 min (transmembrane). Proteins were  
321 resolved on 4-12,5% NuPAGE gels. Dried gels were exposed to Phosphorimager plates, and the  
322 signal acquired with a Typhoon PhosphorImager (GE Healthcare).

### 323 **Detection of Sec61 Interactors in Radiolabeled Membranes**

324 Crude radiolabeled ER vesicles (10 μl) were crosslinked as described in "Chemical Crosslinking"  
325 and submitted to two consecutive immunoprecipitations. Hinge mutants are derived from a *SEC61*  
326 background. Microsomes from the *sec61S353C* strain were included, because Sec61-Mpd1 interac-  
327 tion was first detected in this strain. Crosslinker selection: The Sec61-Mpd1 crosslinked peptide  
328 was first identified by SMPH crosslinking to Sec61S353C. SMPH and LC-SPDP have one cysteine-  
329 and one NH<sub>2</sub>-reactive group. Only LC-SPDP is cleavable, so in the double immunoprecipitation  
330 experiment, SMPH is the negative control for LC-SPDP, because there should be no release of Mpd1  
331 from Sec61 after the first precipitation. SDAD is also cleavable, but with one NH<sub>2</sub>-reactive and one  
332 photoactivatable reactive group. It was used to efficiently crosslink Mpd1 to Sec61 regardless of  
333 the cysteine in loop 7. For the first precipitation, the membranes were solubilized in Lysis Buffer (20  
334 mM Tris, pH 7.5, 2% SDS, 1 mM PMSF) and denatured at 65°C for 10 min. Proteins were then diluted  
335 in Washing Buffer (15 mM Tris-HCl, pH 7.5, 150 mM NaCl, 1% Triton X-100, 2 mM NaN<sub>3</sub>, 1 mM  
336 PMSF). After pre-clearing (as previously), 60 μl of 20% Protein A-Sepharose beads (GE Healthcare)  
337 and appropriate amount of Sec61 antibody was added. Samples were then incubated with rotation  
338 overnight at 4°C, and Protein A Sepharose pellets washed as above. For elution we used 20 μl of  
339 20 mM Tris-HCl, pH 7.5, 5% SDS, 50 mM DTT for 15 min room temperature and denaturation for  
340 10 min 65°C. Eluted proteins were then diluted in Washing Buffer and the Mpd1-HA precipitated  
341 using anti-HA polyclonal antibody (BioLegend). Precipitation was done for 2h at room temperature  
342 followed by elution done 2 x Laemmli Buffer, 200 mM DTT. Proteins were denatured again as before,  
343 resolved on 4-12,5% NuPAGE gels exposed to Phosphorimager plates, and the signal acquired with  
344 a Typhoon PhosphorImager (GE Healthcare).

### 345 **Acknowledgments**

346 We thank Rainer Pepperkok (EMBL Heidelberg) for access to the EMBL Mass Spectrometry facility;  
347 Alexander Leitner (ETH Zürich) for help with xQuest/xProphet and data interpretation; Alexander  
348 Stein and Tom Rapoport (Howard Hughes Medical School), Randy Schekman (UC Berkeley), Randy  
349 Hampton (UC San Diego), Thomas Sommer & Ernst Jarosch (MDC Berlin), Davis Ng (TLL Singapore),  
350 Michael Knop (ZMBH Heidelberg), Pedro Carvalho (Oxford University) for antibodies and plasmids;  
351 Maya Schuldiner (Weizmann Institute) for advice on identifying interesting Sec61 interactors and

352 unpublished information about several of these; Timo Scheller (Saarland University IT) for helping  
353 with xQuest/xProphet pipeline setup; Carmen Clemens for technical assistance.

### 354 **Funding**

355 This work was supported by Saarland University core funding to Karin Römisch and by BBSRC  
356 funding to Ian Collinson (BB/M003604/1 and BB/N015126/1).

### 357 **Contributions**

358 Contributions for this paper were as follow:

- 359 • Fábio Pereira performed and conceived experiments, analyzed results, and wrote the manuscript.
- 360 • Mandy Rettel and Mikhail M. Savitski performed mass spectrometry experiments.
- 361 • Frank Stein performed the statistical analysis of all mass spectrometry data.
- 362 • Ian Collinson designed deletion mutants in loop5 of Sec61.
- 363 • Karin Römisch conceived experiments, analyzed results, wrote the manuscript.

### 364 **References**

- 365 **Aiyar A**, Xiang Y, Leis J. Site-directed mutagenesis using overlap extension PCR. *Methods Mol Biol.* 1996;  
366 57:177–91. doi: [10.1385/0-89603-332-5:177](https://doi.org/10.1385/0-89603-332-5:177).
- 367 **Aviram N**, Ast T, Costa EA, Arakel EC, Chuartzman SG, Jan CH, Haßdenteufel S, Dudek J, Jung M, Schorr S,  
368 Zimmermann R, Schwappach B, Weissman JS, Schuldiner M. The SND proteins constitute an alternative  
369 targeting route to the endoplasmic reticulum. *Nature.* 2016 11; 540(7631):134–138. doi: [10.1038/nature20169](https://doi.org/10.1038/nature20169).
- 370 **Baker RT**, Tobias JW, Varshavsky A. Ubiquitin-specific proteases of *Saccharomyces cerevisiae*. Cloning of UBP2  
371 and UBP3, and functional analysis of the UBP gene family. *J Biol Chem.* 1992 Nov; 267(32):23364–75.
- 372 **Brodsky JL**, Goekeler J, Schekman R. BiP and Sec63p are required for both co- and posttranslational protein  
373 translocation into the yeast endoplasmic reticulum. *Proc Natl Acad Sci U S A.* 1995 Oct; 92(21):9643–6.
- 374 **Carvalho P**, Goder V, Rapoport TA. Distinct ubiquitin-ligase complexes define convergent pathways for the  
375 degradation of ER proteins. *Cell.* 2006 Jul; 126(2):361–73. doi: [10.1016/j.cell.2006.05.043](https://doi.org/10.1016/j.cell.2006.05.043).
- 376 **Christianson JC**, Olzmann JA, Shaler TA, Sowa ME, Bennett EJ, Richter CM, Tyler RE, Greenblatt EJ, Harper JW,  
377 Kopito RR. Defining human ERAD networks through an integrative mapping strategy. *Nat Cell Biol.* 2011 Nov;  
378 14(1):93–105. doi: [10.1038/ncb2383](https://doi.org/10.1038/ncb2383).
- 379 **Cox J**, Mann M. MaxQuant enables high peptide identification rates, individualized p.p.b.-range mass accuracies  
380 and proteome-wide protein quantification. *Nat Biotechnol.* 2008 Dec; 26(12):1367–72. doi: [10.1038/nbt.1511](https://doi.org/10.1038/nbt.1511).
- 381 **Esnault Y**, Feldheim D, Blondel MO, Schekman R, Képès F. SSS1 encodes a stabilizing component of the Sec61  
382 subcomplex of the yeast protein translocation apparatus. *J Biol Chem.* 1994 Nov; 269(44):27478–85.
- 383 **Foresti O**, Rodriguez-Vaello V, Funaya C, Carvalho P. Quality control of inner nuclear membrane proteins by the  
384 Asi complex. *Science.* 2014 Nov; 346(6210):751–5. doi: [10.1126/science.1255638](https://doi.org/10.1126/science.1255638).
- 385 **Gatto L**, Lilley KS. MSnbase-an R/Bioconductor package for isobaric tagged mass spectrometry data visualization,  
386 processing and quantitation. *Bioinformatics.* 2012 Jan; 28(2):288–9. doi: [10.1093/bioinformatics/btr645](https://doi.org/10.1093/bioinformatics/btr645).
- 387 **Ghaemmaghami S**, Huh WK, Bower K, Howson RW, Belle A, Dephoure N, O’Shea EK, Weissman JS. Global  
388 analysis of protein expression in yeast. *Nature.* 2003 Oct; 425(6959):737–41. doi: [10.1038/nature02046](https://doi.org/10.1038/nature02046).
- 389 **Gillece P**, Luz JM, Lennarz WJ, de La Cruz FJ, Römisch K. Export of a cysteine-free misfolded secretory protein  
390 from the endoplasmic reticulum for degradation requires interaction with protein disulfide isomerase. *J Cell*  
391 *Biol.* 1999 Dec; 147(7):1443–56.
- 392 **Grubb S**, Guo L, Fisher EA, Brodsky JL. Protein disulfide isomerases contribute differentially to the endoplasmic  
393 reticulum-associated degradation of apolipoprotein B and other substrates. *Mol Biol Cell.* 2012 Feb; 23(4):520–  
394 32. doi: [10.1091/mbc.E11-08-0704](https://doi.org/10.1091/mbc.E11-08-0704).
- 395 **Horton RM**, Hunt HD, Ho SN, Pullen JK, Pease LR. Engineering hybrid genes without the use of restriction  
396 enzymes: gene splicing by overlap extension. *Gene.* 1989 Apr; 77(1):61–8.

- 397 **Huber W**, von Heydebreck A, Sülthmann H, Poustka A, Vingron M. Variance stabilization applied to microarray  
398 data calibration and to the quantification of differential expression. *Bioinformatics*. 2002; 18 Suppl 1:S96–104.
- 399 **Jadhav B**, McKenna M, Johnson N, High S, Sinning I, Pool MR. Mammalian SRP receptor switches the  
400 Sec61 translocase from Sec62 to SRP-dependent translocation. *Nat Commun*. 2015 Dec; 6:10133. doi:  
401 10.1038/ncomms10133.
- 402 **Janke C**, Magiera MM, Rathfelder N, Taxis C, Reber S, Maekawa H, Moreno-Borchart A, Doenges G, Schwob E,  
403 Schiebel E, Knop M. A versatile toolbox for PCR-based tagging of yeast genes: new fluorescent proteins, more  
404 markers and promoter substitution cassettes. *Yeast*. 2004 Aug; 21(11):947–62. doi: 10.1002/yea.1142.
- 405 **Johnson AE**, van Waes MA. The translocon: a dynamic gateway at the ER membrane. *Annu Rev Cell Dev Biol*.  
406 1999; 15:799–842. doi: 10.1146/annurev.cellbio.15.1.799.
- 407 **Kaiser ML**, Römisch K. Proteasome 19S RP binding to the Sec61 channel plays a key role in ERAD. *PLoS One*.  
408 2015; 10(2):e0117260. doi: 10.1371/journal.pone.0117260.
- 409 **Kalies KU**, Görlich D, Rapoport TA. Binding of ribosomes to the rough endoplasmic reticulum mediated by the  
410 Sec61p-complex. *J Cell Biol*. 1994 Aug; 126(4):925–34.
- 411 **Kalies KU**, Rapoport TA, Hartmann E. The beta subunit of the Sec61 complex facilitates cotranslational protein  
412 transport and interacts with the signal peptidase during translocation. *J Cell Biol*. 1998 May; 141(4):887–94.
- 413 **Kulak NA**, Pichler G, Paron I, Nagaraj N, Mann M. Minimal, encapsulated proteomic-sample processing applied to  
414 copy-number estimation in eukaryotic cells. *Nat Methods*. 2014 Mar; 11(3):319–24. doi: 10.1038/nmeth.2834.
- 415 **Leitner A**, Walzthoeni T, Aebersold R. Lysine-specific chemical cross-linking of protein complexes and identifica-  
416 tion of cross-linking sites using LC-MS/MS and the xQuest/xProphet software pipeline. *Nat Protoc*. 2014 Jan;  
417 9(1):120–37. doi: 10.1038/nprot.2013.168.
- 418 **Mehnert M**, Sommer T, Jarosch E. Der1 promotes movement of misfolded proteins through the endoplasmic  
419 reticulum membrane. *Nat Cell Biol*. 2014 Jan; 16(1):77–86. doi: 10.1038/ncb2882.
- 420 **Neal S**, Jaeger PA, Duttke SH, Benner C, K Glass C, Ideker T, Hampton RY. The Dfm1 Derlin Is Required  
421 for ERAD Retrotranslocation of Integral Membrane Proteins. *Mol Cell*. 2018 Jan; 69(2):306–320.e4. doi:  
422 10.1016/j.molcel.2017.12.012.
- 423 **Ng W**, Sergeyenko T, Zeng N, Brown JD, Römisch K. Characterization of the proteasome interaction with the  
424 Sec61 channel in the endoplasmic reticulum. *J Cell Sci*. 2007 Feb; 120(Pt 4):682–91. doi: 10.1242/jcs.03351.
- 425 **Pilla E**, Schneider K, Bertolotti A. Coping with Protein Quality Control Failure. *Annu Rev Cell Dev Biol*. 2017 10;  
426 33:439–465. doi: 10.1146/annurev-cellbio-111315-125334.
- 427 **Pilon M**, Schekman R, Römisch K. Sec61p mediates export of a misfolded secretory protein from the endoplasmic  
428 reticulum to the cytosol for degradation. *EMBO J*. 1997 Aug; 16(15):4540–8. doi: 10.1093/emboj/16.15.4540.
- 429 **Ritchie ME**, Phipson B, Wu D, Hu Y, Law CW, Shi W, Smyth GK. limma powers differential expression analyses  
430 for RNA-sequencing and microarray studies. *Nucleic Acids Res*. 2015 Apr; 43(7):e47. doi: 10.1093/nar/gkv007.
- 431 **Römisch K**. Endoplasmic reticulum-associated degradation. *Annu Rev Cell Dev Biol*. 2005; 21:435–56. doi:  
432 10.1146/annurev.cellbio.21.012704.133250.
- 433 **Römisch K**. A Case for Sec61 Channel Involvement in ERAD. *Trends Biochem Sci*. 2017 03; 42(3):171–179. doi:  
434 10.1016/j.tibs.2016.10.005.
- 435 **Savitski MM**, Reinhard FBM, Franken H, Werner T, Savitski MF, Eberhard D, Martinez Molina D, Jafari R, Dovega  
436 RB, Klaeger S, Kuster B, Nordlund P, Bantscheff M, Drewes G. Tracking cancer drugs in living cells by thermal  
437 profiling of the proteome. *Science*. 2014 Oct; 346(6205):1255784. doi: 10.1126/science.1255784.
- 438 **Schäfer A**, Wolf DH. Sec61p is part of the endoplasmic reticulum-associated degradation machinery. *EMBO J*.  
439 2009 Oct; 28(19):2874–84. doi: 10.1038/emboj.2009.231.
- 440 **Schäuble N**, Lang S, Jung M, Cappel S, Schorr S, Ulucan Ö, Linxweiler J, Dudek J, Blum R, Helms V, Paton AW,  
441 Paton JC, Cavalié A, Zimmermann R. BiP-mediated closing of the Sec61 channel limits Ca<sup>2+</sup> leakage from the  
442 ER. *EMBO J*. 2012 Aug; 31(15):3282–96. doi: 10.1038/emboj.2012.189.

- 443 **Scheper W**, Thaminy S, Kais S, Stagljar I, Römisch K. Coordination of N-glycosylation and protein translocation  
444 across the endoplasmic reticulum membrane by Sss1 protein. *J Biol Chem.* 2003 Sep; 278(39):37998–8003.  
445 doi: [10.1074/jbc.M300176200](https://doi.org/10.1074/jbc.M300176200).
- 446 **Schwanhäusser B**, Busse D, Li N, Dittmar G, Schuchhardt J, Wolf J, Chen W, Selbach M. Global quantification of  
447 mammalian gene expression control. *Nature.* 2011 May; 473(7347):337–42. doi: [10.1038/nature10098](https://doi.org/10.1038/nature10098).
- 448 **Servas C**, Römisch K. The Sec63p J-domain is required for ERAD of soluble proteins in yeast. *PLoS One.* 2013;  
449 8(12):e82058. doi: [10.1371/journal.pone.0082058](https://doi.org/10.1371/journal.pone.0082058).
- 450 **Shamu CE**, Walter P. Oligomerization and phosphorylation of the Ire1p kinase during intracellular signaling  
451 from the endoplasmic reticulum to the nucleus. *EMBO J.* 1996 Jun; 15(12):3028–39.
- 452 **Sikorski RS**, Hieter P. A system of shuttle vectors and yeast host strains designed for efficient manipulation of  
453 DNA in *Saccharomyces cerevisiae*. *Genetics.* 1989 May; 122(1):19–27.
- 454 **Stein A**, Ruggiano A, Carvalho P, Rapoport TA. Key steps in ERAD of luminal ER proteins reconstituted with  
455 purified components. *Cell.* 2014 Sep; 158(6):1375–1388. doi: [10.1016/j.cell.2014.07.050](https://doi.org/10.1016/j.cell.2014.07.050).
- 456 **Stirling CJ**, Rothblatt J, Hosobuchi M, Deshaies R, Schekman R. Protein translocation mutants defective in the  
457 insertion of integral membrane proteins into the endoplasmic reticulum. *Mol Biol Cell.* 1992 Feb; 3(2):129–42.  
458 doi: [10.1091/mbc.3.2.129](https://doi.org/10.1091/mbc.3.2.129).
- 459 **Tretter T**, Pereira FP, Ulucan O, Helms V, Allan S, Kalies KU, Römisch K. ERAD and protein import defects in a  
460 sec61 mutant lacking ER-lumenal loop 7. *BMC Cell Biol.* 2013 Dec; 14:56. doi: [10.1186/1471-2121-14-56](https://doi.org/10.1186/1471-2121-14-56).
- 461 **Vashist S**, Ng DTW. Misfolded proteins are sorted by a sequential checkpoint mechanism of ER quality control. *J*  
462 *Cell Biol.* 2004 Apr; 165(1):41–52. doi: [10.1083/jcb.200309132](https://doi.org/10.1083/jcb.200309132).
- 463 **Vembar SS**, Brodsky JL. One step at a time: endoplasmic reticulum-associated degradation. *Nat Rev Mol Cell*  
464 *Biol.* 2008 Dec; 9(12):944–57. doi: [10.1038/nrm2546](https://doi.org/10.1038/nrm2546).
- 465 **Voorhees RM**, Hegde RS. Structure of the Sec61 channel opened by a signal sequence. *Science.* 2016 Jan;  
466 351(6268):88–91. doi: [10.1126/science.aad4992](https://doi.org/10.1126/science.aad4992).
- 467 **Walter P**, Ibrahimi I, Blobel G. Translocation of proteins across the endoplasmic reticulum. I. Signal recognition  
468 protein (SRP) binds to in-vitro-assembled polysomes synthesizing secretory protein. *J Cell Biol.* 1981 Nov; 91(2  
469 Pt 1):545–50.
- 470 **Wang L**, Dobberstein B. Oligomeric complexes involved in translocation of proteins across the membrane of  
471 the endoplasmic reticulum. *FEBS Lett.* 1999 Sep; 457(3):316–22.



## Supplemental Figures

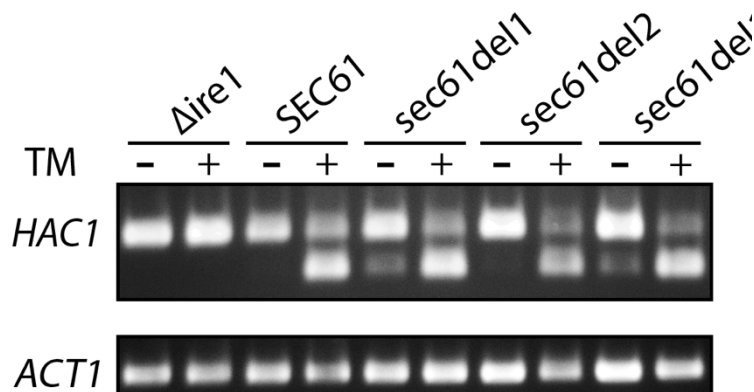


**Figure 3 – Figure supplement 1 – HAC1 mRNA Splicing Assay to evaluate UPR induction.** Wildtype and Sec61 hinge mutants were either treated with tunicamycin (2  $\mu\text{g/ml}$ ) (TM) or DMSO (control), followed by total RNA isolation, and cDNA production from isolated RNA. A quantitative PCR was done from equal amounts of cDNA. Agarose gel showing the resultant PCR products. Upper slice shows HAC1 PCR product. Upper bands (720 bp) represent the unspliced (uninduced) HAC1 mRNA, while lower bands (470 bp) represent the spliced (induced) HAC1 mRNA. Bottom slice show the actin PCR product. The  $\Delta ire1$  mutant was used as negative control.

## Supplemental Methods

### RNA isolation and HAC splicing PCR

For the isolation of RNA all solutions were RNase free. Strains to be evaluated were grown to an  $\text{OD}_{600}=1$ , and two 10 ml replicas per strain were made. To one replica tunicamycin (2  $\mu\text{g/ml}$  of) was added, to the other DMSO (same volume as tunicamycin), and cells were grown for 3h more. Cells were then harvest at 4,500 x g for 5 min (4°C), resuspended in 1 ml ice-cold DEPC-water, and transferred to an RNase-free tube. After sedimentation (13,000 x g, 10 sec, 4°C) pellet was resuspended in 400  $\mu\text{l}$  TES Solution (10 mM Tris-HCl, pH 7.7, 10 mM EDTA, 0.5% (w/v) SDS), 400  $\mu\text{l}$  of Roti-Aqua-Phenol® (Carl Roth) were added, and after vortexing (10 sec), samples were incubated for 1 h at 65°C with occasional vortexing. Samples were then placed on ice for 5 min and centrifuged at 13,000 x g for 5 min (4°C). Aqueous phase was transferred to a clean tube and 400  $\mu\text{l}$  of Roti-Aqua-Phenol® were added. Samples were vortexed for 20 sec and incubated for 5 min on ice. Samples were then centrifuged as before, aqueous phase transferred again to a clean tube, and 400  $\mu\text{l}$  of chloroform were added. Samples were vortexed again (20sec) and sedimented (13,000 x g, 5 min, 4°C). Aqueous phase was once more transferred to a clean tube, and 40  $\mu\text{l}$  of 3M NaAc, followed by 1 ml of ice cold 100% ethanol, were added. After repeating the vortexing and sedimentation steps, pellets were washed with 1.5 ml of 70% ethanol and sedimented as before. Finally, samples were resuspended in 50  $\mu\text{L}$  of DEPC-water and RNA concentration was determined using a NanoDrop spectrophotometer (ThermoFisher).

To generate cDNA from each RNA samples, the RNA samples were diluted to a concentration of 0.1  $\mu\text{g/ml}$  and reverse-transcription reactions were made as follows using MaximaRT® (ThermoFisher):

Component	Volume ( $\mu$ l)	Final concentration
RNA	1	0.1 $\mu$ g
Oligo(dT18)-primer (100 mM)	1	100 pmol
dNTP mix (10 mM)	1	0.5 mM
RNase-free dH <sub>2</sub> O	To 14.5	to 14.5 $\mu$ l
5X RT buffer	4	1x
RNasin (40 U/ $\mu$ l)	0.5	20 U
Maxima <sup>®</sup> RT	1	200 U

Samples were then incubated for 30min at 50°C followed by an inactivation at 85°C for 5 min. We then used 1  $\mu$ l of each cDNA for PCR, using both the *HAC1*- (5'-CTGGCTGACCACGAAGAC and 5'-TTGTCTTCATGAAGTGATGGC-3') and the *ACT1*- (5'-ATTCTGAGGTTGCTGCTTT-3' and 5'-GTGGTGAACGATAGATGG-3') specific primers.

Amplification reactions were done using KAPAHiFi™ Hot Start DNA (PEQLAB) and the program used was the following:

Cycles	Step	Temperature	Duration
1	Initial denaturation	95	5 sec
35	Denaturation	98	20 sec
	Annealing	54	15 sec
	Extension	72	30 sec/kb
1	Final Extension	72	5 min
	Store	4	$\infty$

After PCR 10  $\mu$ l of each reaction was resolved in an 1% agarose gel at 100V for 1h. Signal was acquired with the E-BOX VX2 gel documentation system (PEQLAB).